Biochar-based engineered composites for sorptive decontamination of water: A review

K.S.D. Premarathna[a], Anushka Upamali Rajapaksha[a], Binoy Sarkar[b], Eilhann E. Kwon[c], Amit Bhatnagar[d], Yong Sik Ok[e,**], Meththika Vithanage[a,f,*]

[a] Ecosphere Resilience Research Center, Faculty of Applied Sciences, University of Sri Jayewardenepura, Nugegoda 10250, Sri Lanka
[b] Department of Animal and Plant Sciences, The University of Sheffield, Sheffield S10 2TN, UK
[c] Department of Environment and Energy, Sejong University, 98 Gunja-Don, Republic of Korea
[d] Department of Environmental and Biological Sciences, University of Eastern Finland, P.O. Box 1627, FI-70211 Kuopio, Finland
[e] Korea Biochar Research Center, O-Jeong Eco-Resilience Institute (OJERI) & Division of Environmental Science and Ecological Engineering, Korea University, Seoul 02841, Republic of Korea
[f] Molecular Microbiology and Human Diseases Project, National Institute of Fundamental Studies, Kandy, Sri Lanka

HIGHLIGHTS

- Biochar composites for improved water pollution abatement are reviewed.
- Metals and metal oxides have been widely used in engineered biochar.
- Modification typically alters the surface properties and functionalities of biochar.

GRAPHICAL ABSTRACT

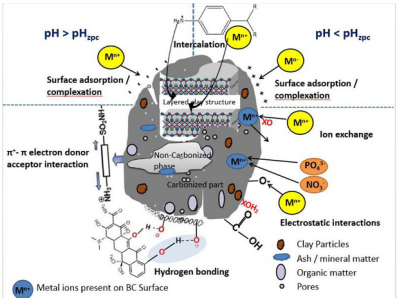

ARTICLE INFO

Keywords:
Adsorption
Water pollution
Trace metals
Antibiotics
Biochar
Nutrients
Clay minerals

ABSTRACT

Biochar (BC) exhibits a great potential as an adsorbent in decontamination of water. To improve the adsorption capabilities and impart the particular functionalities of BC, various methods (chemical modification, physical modification, impregnation with different materials, and magnetic modification) have been developed. As compared to surface modifications, BC-based composites provide various technical and environmental benefits because they require fewer chemicals, lesser energy, and confer enhanced contaminant removal capacity. Therefore, this review focuses on BC composites prepared by the combination of BC with different additives including metals, metal oxides, clay minerals, and carbonaceous materials, which greatly alter the physicochemical properties of BC and broaden its adsorption potential for a wide range of aquatic contaminants. Techniques for the preparation of BC composites, their adsorption potentials for a variety of inorganic and organic environmental contaminants, factors affecting BC properties and the adsorption process, and the mechanisms involved in adsorption are also discussed. Modification typically alters the surface properties and functionalities of BC composites including surface area, pore volume, pore size, surface charge, and surface functional groups. Hence, modification enhances the adsorption capacity of BC for most organic and inorganic compounds and ions. Nevertheless, some modifications negatively affect the adsorption of certain contaminants because of various factors including obstruction of pores due to over coating and development of same charge as

contaminant on the surface of BC. However, the use of BC composites in environmental remediation is still in its infancy, and further research and development is needed to reach scalability and commercialization of the new technology.

1. Introduction

Biochar (BCs) is defined as a carbon-rich material obtained by the thermal treatment of carbon neutral carbonaceous materials such as wood, manure, or leaves under an oxygen free environment [1]. It has garnered attention due to its genuine physico-chemical properties and diverse applications in many sectors, including agriculture, climate change mitigation, energy production, and environmental remediation [2]. The addition of BC to soil improves soil fertility, enhances agricultural productivity, increases soil nutrient levels and water holding capacity, and reduces emissions of greenhouse gases due to its intrinsic carbon negativity [1]. However, the use of BC as a sustainable medium in such applications has only been studied scientifically in the last decade [3]. Recent uses of BC involve as a carbon precursor for catalysts and contaminant adsorbents, as a gas adsorbent, as an energy source in fuel cell systems, and as a raw material in supercapacitor and activated carbon production [3,4]. These high value applications are still in their early stages, and further research and development is needed to achieve their scalability and commercialization.

Biochar can be produced using various carbonaceous feedstocks, many of which are considered organic wastes, thereby indirectly supporting waste management. Because of its low production cost and feasibility in many contexts [5], it has been used in wastewater treatment as a low-cost adsorbent alternative to activated carbon (AC) for the removal of various contaminants from water such as nutrients, trace metals, pharmaceuticals, pesticides, dyes, metal(loids), volatile organic compounds and polycyclic aromatic hydrocarbons [6–11].

The methods for producing BC from carbonaceous materials (mostly biomass) are pyrolysis, and hydrothermal carbonization [2]. The yield of BC from these processes differs based on operational conditions, types of biomass, and reaction media [3]. The most frequently used method is pyrolysis, which can be categorized into slow and fast pyrolysis depending on the pyrolysis temperature, heating rate, and residence time employed; each operation parameters impart different characteristics to the final BC products (Table 1) [12,13].

Recent consideration for BC research was due to its close similarities in performance capacity to AC in many uses. Generally AC has greater Brunauer–Emmett–Teller (BET) surface area, surface activity, porosity, and physicochemical stability than BC [14]. The BET surface areas of AC produced from mill and forest residues via steam activation in a rotary calciner at 815 °C (1283.0 $m^2 g^{-1}$ and 575.9 $m^2 g^{-1}$, respectively) were significantly higher than those of BC produced using the same feedstocks using gasification system designed by Tucker Engineering Associates (TEA) (15.0 $m^2 g^{-1}$ and 11.8 $m^2 g^{-1}$, respectively) [15]. Similar trend was shown regarding pore volume and total porosity. As a result of this, AC is being studied as the most prominent environmental media for the removal of different environmental contaminants via adsorption (Fig. 1).

Despite the fact that AC is a successful adsorbent, one of the demerits for being used as adsorbent is its high production cost and

Table 1
Pathways for thermal conversion of biomass to biochar.

Thermal conversion process	Temperature range (°C)	Heating rate	Residence time	Biochar yield %
Slow pyrolysis	350–800	Slow, (< 10 °C min^{-1})	Hours–Days	35
Fast pyrolysis	400–600	Very fast (1000 °C s^{-1})	Seconds	10–15
Hydrothermal carbonization	180–250	Slow (< 10 °C min^{-1})	Hours	30–60

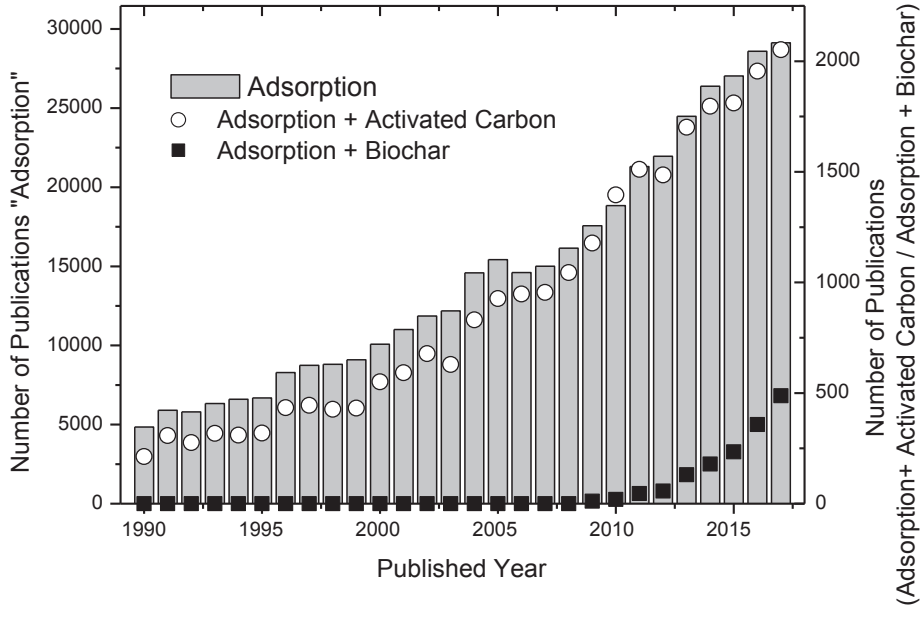

Fig. 1. Science Citation Indexed publications on adsorption and adsorption related to activated carbon and biochar in SCOPUS (Accessed on 2018.01.10).

difficulties with regeneration [16]. According to the literature, the estimated cost for BC and AC are USD 246 t^{-1}, and USD 1500 t^{-1}, respectively, which means that BC is approximately 1/6 less expensive than AC [17], and the choice of the initial feedstock for biochar production is more flexible than that of AC. In these respects, BC has been vital as a low-cost adsorbent alternative to AC [16]. However, compared to AC, it has not been promising in the context of sorptive removal of contaminants because of its relatively low surface area and the influence of abiotic and/or biotic processes on its properties and adsorption capacity for contaminants [15]. Therefore, a great deal of researches has focused on enhancing the surface area and mechanical properties of BC through diverse modification methods, i.e. chemical, physical and magnetic modification and impregnation with mineral sorbents [18].

Engineered BCs prepared via impregnation with minerals are referred to as BC composites. These composites can be prepared by incorporating BC with metal oxides, clay minerals, organic compounds, or carbonaceous materials such as graphene oxide (GO), polysaccharides, and carbon nanotubes (CNT), all of which greatly alter the surface functionalities of the BC [19,20]. In these composites, BC acts as a porous structure to support the distribution of modifier particles/compounds within its matrix and enhances the adsorption capacity for a wide range of contaminants [21]. In some instances, the unwanted functionalities were imparted during the fabrication of BC composites such as reduction of adsorption capacity via obstruction of pores [22,23]. Hence, it is desirable to evaluate both the positive and negative impacts of BC modification on adsorption of target adsorbates.

Production of BCs and the characterization of their properties and adsorption capacities for various contaminants have been thoroughly reviewed [5,12,24–26]. Although numerous studies have been published on the adsorption efficiencies of BCs, attention to engineered/"designer" BCs for contaminant remediation has not been fully matured [2,18,19,27] (Table 2). Most reviews have focused on the removal capacities, while less (or no) attention was given to a mechanistic understanding of the removal, despite this being of equal importance since adsorption is a micro-molecular level process. Therefore, the overarching objective of this review is to compensate the knowledge gap surrounding pristine and engineered/designer BCs and their properties and uses, by revisiting the literature published within the last decade (2007 to 2018). This review provides a comprehensive summary of the environmental applications of various BC composites and important factors that influence the characteristics of BCs, as well as discusses the factors influencing adsorption and mechanisms involved in the adsorption process.

2. Pristine biochar: State-of-the-art adsorbent

Biochar is a carbon-rich material obtained by the thermal treatment of carbon neutral carbonaceous materials such as wood, manure, or leaves under an oxygen free environment Biochar is produced through the dry carbonization or pyrolysis of biomass, differing from both charcoal (complete carbonization) and hydrochar (which is produced as slurry in water via hydrothermal carbonization of biomass under pressure). Feedstocks used for the production of BC can be divided into two categories: produced biomass and its by products, and waste biomass [39,40]. Animal manure, municipal solid waste (MSW), woody biomass, and crop residues are commonly employed as waste feedstocks [5]. Waste materials are a very cost-effective feedstock because they are abundant and easily collectable, and further indirectly support waste management and carbon neutrality in urban/rural areas.

2.1. Factors influencing properties of biochar

The characteristics of BC are highly contingent on the types of feedstock, pyrolytic temperature, heating rate, reaction media, and residence time [19]. Biochar from animal litter and solid waste result in

Table 2
Reviews published based on the applications of biochar in the removal of different types of contaminants available in aqueous media.

Title of review	Anions	Cations	Pharmaceuticals	Dyes	PAHs	VOCs	Agrochemicals	Reference
Interaction of arsenic with biochar in soil and water: A critical review	√							Vithanage et al. [28]
Biochar-based removal of antibiotic sulfonamides and tetracyclines in aquatic environments: A critical review			√					Peiris et al. [25]
Biochar adsorption treatment for typical pollutants removal in livestock wastewater: A review	√	√	√	√			√	Deng et al. [29]
Environmental application of biochar: Current status and perspectives			√	√	√	√	√	Oliveira et al. [30]
Biochar as a low-cost adsorbent for heavy metal removal: A review		√						Patra et al. [31]
A review of biochar as a low-cost adsorbent for aqueous heavy metal removal		√						Inyang et al. [24]
Application of biochar for the removal of pollutants from aqueous solutions		√	√	√				Tan et al. [32]
Characteristics and applications of biochar for environmental remediation: A review	√	√			√			Xie et al. [33]
Biochar preparation, characterization, and adsorptive capacity and its effect on bioavailability of contaminants: An overview		√	√		√			Nartey and Zhao [34]
Organic and inorganic contaminants removal from water with biochar, a renewable, low-cost and sustainable adsorbent – A critical review	√	√		√	√		√	Mohan et al. [12]
Biochar as a sorbent for contaminant management in soil and water: A review			√	√	√		√	Ahmad et al. [5]
Characterization and adsorption capacities of low-cost sorbents for waste water treatment – A review	√	√						Gisi and Notarnicola [35]
A review: Utilization of biochar for waste water treatment	√	√	√	√			√	Zhang et al. [36]
The potential role of biochar in the removal of organic and microbial contaminants from potable and reuse water: A review	√	√	√	√				Inyang and Dickenson [37]
Challenges and recent advances in biochar as low-cost biosorbent: From batch assays to continuous-flow systems	√	√	√	√				Rosales et al. [38]

high yields and ash contents compared to those produced from crop residues and wood [41], because of the high content of inorganic constituents [5,42]. The presence of various innate metals in animal litter also increases the BC yield by preventing the loss of volatile material through changing the bond dissociation energies of organic and inorganic carbon bonds [43]. Ash content is also affected by the composition of the feedstock; high ash contents were found in animal manure and waste BCs owing to the high labile and volatile C contents in these biomasses [41]. For example, BC from chicken manure contains more than 17.5 wt% of ash content [44]. Animal manure-derived BC has a higher mineral content than that derived from plant matter [41]. Even at high pyrolysis temperatures (> 700 °C), BC produced from animal excreta and solid waste exhibit relatively lower surface areas than those produced from crop residues and woods [5]. This is due to the extensive cross-linking that results from the lower C contents and high molar ratios of H/C and O/C in crop residues and wood feedstocks [45]. Moreover, the collapse of structural matrix of lignocellulose biomass via the digestion system (i.e., acidic conditions and biological fermentation) is one of the factors lowering the surface area of BC [46].

In general, the yield of BC decreases with increasing pyrolysis temperature, which is likely due to the degree of carbonization [47]. At 400 °C, BC produced from wheat straw (WS-BC), corn straw (CS-BC), and peanut shell (PS-BC) achieved yields of 32.4, 35.5, and 36.8 wt%, respectively; upon increasing the temperature to 700 °C, these yields decreased to 22.8, 24.9, and 25.8%, respectively [48]. The yield of BC produced from vermicompost (VM-BC) also achieved higher yield at 400 °C (91.56 wt%) than at 700 °C (71.81 wt%) [49]. This was mainly due to the destruction of cellulose and hemicellulose as well as the thermolysis of organic materials at high pyrolysis temperatures [50]. At higher pyrolysis temperatures, C and ash contents significantly increase due to thermal cracking of volatile fraction in biomass and its subsequent carbonization [51,52]. Ash content of bamboo based BC (BB-BC) increased from 14.38 to 26.34 wt% on increasing the temperature from 250 to 550 °C, and VM-BC exhibited a 18.23 wt% increase in ash content when the temperature was increased from 300 to 700 °C [49,52].

The low H/C molar ratio obtained at higher pyrolysis temperatures is likely due to the aromaticity, which makes BC more chemically and biologically stable [51]. The VM-BC and pine needle derived BC (PN-BC) produced at 300 °C contained higher H/C molar ratios (0.13 and 0.62, respectively) than at 700 °C (0.03 and 0.08, respectively) [49,51]. Polarity and surface oxygen functional group density are indicated by the O/C and (O + N)/C molar ratios [53]. The low O/C and (O + N)/C molar ratios obtained at high pyrolysis temperatures reduced the polarity of BC surfaces because they contained fewer surface oxygenated functional groups [49]. The highest O/C and (O + N)/C molar ratios (0.46 and 0.55, respectively) in VM-BC were obtained at 300 °C, and the lowest (0.02 and 0.07, respectively) at 700 °C; for PN-BC, the highest O/C molar ratio (0.07) was also obtained at 700 °C [49,51]. An increase in pH occurs at higher pyrolysis temperatures due to the retention of a higher number of alkaline groups, the separation of alkali salts (K, Na, Ca, and Mg) from organic compounds, and the removal of acidic functional groups [54,55]. For example, the pH of VM-BC increased from 7.37 to 11.31 upon an increase in temperature from 300 to 700 °C [49].

Surface area and pore volume also increase with increasing temperature [49,56] because of the recombination and crystallization of C during the carbonization step [57]. The surface area of VM-BC increased 3-fold, and the pore volume also increased from 0.092 to 0.19 mL g^{-1} when the temperature was increased from 300 to 700 °C [49]. The total pore volume of PN-BC was eight times higher at 700 °C than that at 500 °C [51]. Further, the average pore diameters in VM-BC produced at 300, 500, and 700 °C were 15.05, 13.91, and 9.94 nm, respectively, which suggested that the micro-pores are dominantly formed during the carbonization step at temperature higher than 550 °C [49].

2.2. Adsorption properties of biochar

Biochars produced at higher pyrolysis temperatures (700 °C) exhibit higher adsorption capacities for antibiotics as compared to those produced at lower pyrolysis temperatures, however, in some cases, even trace metals adsorption have shown high at high temperature biochars [7,54]. High aromaticity of the high temperature BCs lead to increase the removal capacities of antibiotics, at the same time decrease in polarity supports at high temperatures support the same [54]. Adsorption of trichloroethylene (TCE) mainly occurred via a pore-filling and hydrophobic partitioning mechanisms [51]. Adsorption of TCE was prevented by the oxygenated functional groups left intact in BCs produced at lower pyrolysis temperatures, which instead adsorbed water through hydrogen bonding [58]. Pharmaceuticals typically interact with BC via *Van der Waals* interactions, electrostatic interactions, and hydrogen bonding [59]. Functional group density is higher in BC produced at low pyrolysis temperatures, of which mechanisms for adsorption are mainly explained by electrostatic interactions and hydrogen bonding between BC and the functional groups of target compounds [32]. Biochar produced at higher pyrolysis temperatures has been shown to retain a higher quantity of anionic dyes and a lower quantity of cationic dyes [49]. Adsorption of cationic and anionic dyes occurred via cation exchange and π–π interactions, respectively [49]. Adsorption capacity for pesticides was also increased with increasing pyrolysis temperature [56]. Pesticides interact with BC via strong π–π electron-donor–-acceptor (EDA) interactions, acid-base interactions, amide bond formation, electrophilic addition, covalent bond, ionic and hydrogen bonding, van der Waals forces and hydrophobic interactions [56].

Adsorption of both organic and inorganic compounds on BC is pH-dependent, because the BC surface charge varies according to the point zero charge (pH_{pzc}) of BC. At pH < pH_{pzc}, the surface is negatively charged, which expedites adsorption of positively charged contaminants due to the electrostatic interactions. At pH > pH_{pzc}, the surface is positively charged which prevents adsorption of positively charged compounds due to the electrostatic repulsion [60]. Antibiotics, pesticides and many organic compounds exhibit different pK_a values, and thus, depending on the pH of a given medium, the antibiotic can predominantly exist in its cationic, anionic, or neutral forms [61,62]. At higher pH values, anionic species become the dominant form of some antibiotics such as tetracycline, sulfamethazine, ciprofloxacin etc. The electrostatic repulsion between the negatively charged BC surface and anionic species of antibiotics would thus increase, resulting in decreased adsorption at higher pH values [63]. However, high pH also facilitates weaker π–π EDA interactions between the antibiotic and BC surface [63]. At lower pH conditions, anionic dye adsorption mainly occurs via electrostatic interactions between the negatively charged anionic dye and protonated hydroxyl and carboxylic acid groups of BC [64]. However, adsorption of cationic dyes decreases due to repulsive forces occurring between cationic dyes and positively charged functional groups of BC [49]. At higher pH, protonated functional groups of BC gradually deprotonated, as a result electrostatic interaction weakens, leading to a decrease in the adsorption of anionic dyes but an increase in the adsorption capacity for cationic dyes [49].

3. Engineered biochar composites: preparation methods/ synthesis

This section mainly focuses on the production processes of several key BC composites **(**Fig. 2**).**

3.1. Biochar composites prepared with clay minerals

In recent years, clay minerals have been widely employed in medicine, pharmacy, agriculture, and the manufacturing of cosmetics, paint, and ink [65]. Due to their lamellar structures, high surface area, and high ion-exchange capacities, clay minerals have been effectively

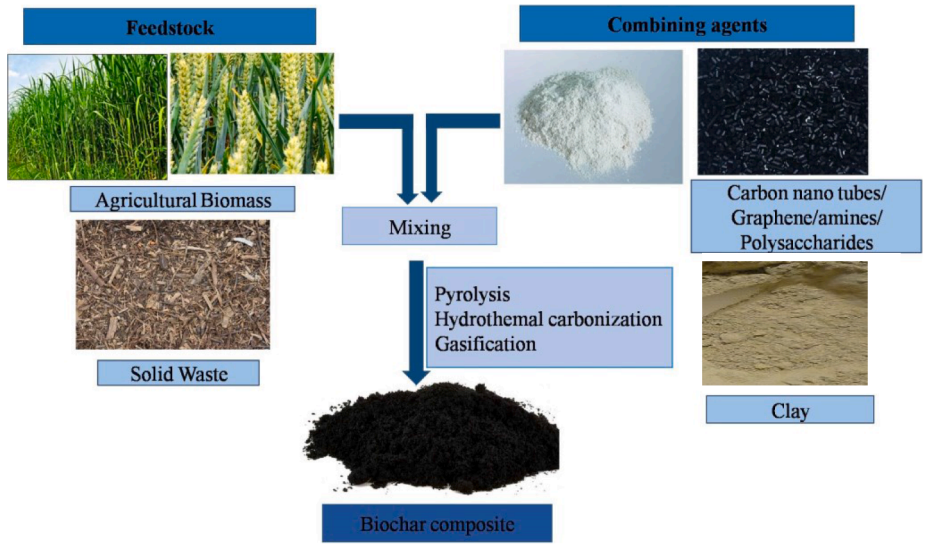

Fig. 2. Engineered biochar composites preparation pathways.

used as adsorbents for the removal of different types of antibiotics, polymers, and heavy metals/metalloids [66–70]. However, exclusive use of clays as adsorbents does not appear to be prospective due to the regeneration issues as well as the volume of residue after adsorption. Clay-BC composites prepared by mixing of small amount of clay with BC has demonstrated promising results and high sorption capacities in removing different contaminants [21]. Although various methods have been used to produce clay–BC composites, the most common ones involve the preparation of a clay–BC slurry for pyrolysis [21,22]. In brief, the feedstock is dipped in a stable clay suspension which is prepared by adding the powdered material to deionized (DI) water or another suitable solvent and pyrolyzed under oxygen-limited conditions in a muffle furnace at the relevant temperature [21]. Alternatively, BC can also directly be soaked in a slurry prepared with clay minerals, deionized water, and acetic acid, stirred overnight, and then oven-dried at 60 °C for 24 h. The most commonly used weight ratios of clay:biomass/BC for both procedures were 1:5, 1:4, 1:2, and 1:1 [21,22,71–73].

3.2. Biochar composites prepared with metals and metal oxides

In BC–metal/metal oxide composites, BC acts as a porous carbon platform upon which metal oxides precipitate, thus increasing the surface area available for adsorption. Generally, impregnation with metal oxides is performed by soaking BCs or their feedstocks in solutions of metal nitrates or chlorides. The most frequently used impregnation agents described in the literature are $FeCl_3$, Fe_2O_3, $Fe(NO_3)_3$, and $MgCl_2$ [74–76]. Preparation of metal oxide composites of BC was done by two methods: pre-pyrolysis treatment, soaking of the biomass followed by pyrolysis; or post-pyrolysis treatment, pyrolysis of the biomass followed by soaking in metal ion solution [18]. In the pre-pyrolysis method, the feedstock is soaked in a metal salt solution and then pyrolyzed under an oxygen-free environment [23]. In the post-pyrolysis method, pyrolysed feedstock is soaked in a metal salt solution [74,77].

3.3. Biochar composites prepared with carbonaceous materials

Biochar can be combined with carbonaceous materials that have functional groups capable of creating strong bonds with both the BC surface and the pollutants present in aqueous medium. Polysaccharides, amines, carbonaceous nanomaterials, and CNTs are the most commonly used agents [78–80]. Such modification can be achieved either through simple chemical reactions or by mixing BC with polymers rich in amino groups such as polyethylenimine or chitosan [81]. Among bulk carbon materials, graphene (G) and carbon nanotubes (CNT) are commonly used in composite synthesis due to their great binding affinity through functionalization with −OH and −COOH groups via chemical oxidation methods [82]. Since the porous structure and relatively high surface area of BCs, it can be used as a host to distribute and stabilize carbon nano-materials and expand the range of potential applications [26]. Modification can further enhance the adsorption capacities of BCs for different toxic pollutants [73,83].

4. Characteristics of biochar composites and their influencing factors

Biochar composites are prepared by combining the carbon neutral feedstock with different types of materials. For the preparation of BC, different feedstocks from a range of agricultural and carbonaceous materials have been used [1]. Characteristics of BC composites mainly depend on characteristics of the feedstock, combining agents and pyrolysis conditions [19]. Table 3 summarizes the characteristics of BC composites produced from different feedstocks under different pyrolysis conditions.

High BC yield may be related to a higher composition of inorganic constituents in feedstock materials [5]. It is suggested that various metals present in animal litter may protect against the loss of volatile material by changing the bond dissociation energies of organic and inorganic carbon bonds [43]. For example, the enhanced dehydrogenation in the presence of inorganic constituents (catalytic effects) generally expedites crystallization, thereby resulting in the high yield of BC. Generally, biomass with high lignin content results in high BC yield [42]. The yield and elemental contents of BC composites decrease with increasing pyrolysis temperature due to greater loss of volatile components [52]. The yield of some BC is generally increased up to a heating rate of 5 °C min^{-1}, but further increases result in decreased yields. With the increase of heating rate, production of bio-crude and bio-gas dominate, resulting in low BC yield due to the breakdown of organic compounds [84]. An increase in residence time slightly decreases BC yield due to greater volatilization during longer pyrolysis conditions [84]. Therefore, clay minerals, metal/metal oxides and carbonaceous modifiers have exhibited strong influence on the yield of BC [52,79]. The ash content of BC is proportional to the pyrolysis temperature [48,83]. The ash content is also varied with the types of biomass feedstocks. Hence, both metal oxide and clay modifications slightly increase the ash content in BC composites compared to raw

Table 3
Characteristics of BC composites produced from different feedstocks at different pyrolysis temperatures.

Feedstock	Modifier	Pyrolysis Temp. and Time	Yield %	pH	C	H	O	N	S	Fe	Al	Ca	Na	K	Mg	Ash	Surface area $m^2 g^{-1}$	Pore volume $cm^3 g^{-1}$	Reference
					%														
Bamboo	Untreated	250 °C 30 min	78.00	–	51.90	5.45	–	0.87	0.08	0.01	–	0.50	–	0.83	–	14.38	–	0.36	Rawal et al.
		350 °C 30 min	60.00	–	71.50	4.02	–	1.11	0.07	0.01	–	0.08	–	1.40	–	28.08	–	1.05	[52]
		450 °C 30 min	35.00	–	75.00	3.42	–	1.38	0.12	0.02	0.01	0.10	–	1.40	–	19.10	–	0.77	
		550 °C 30 min	33.00	–	79.20	2.72	–	1.28	0.06	0.03	0.01	0.08	–	0.85	–	26.34	–	1.01	
	Iron-kaolinite	250 °C 30 min	86.00	–	48.70	5.15	–	0.50	1.00	2.00	0.03	0.05	–	0.74	–	15.43	–	0.73	
		350 °C 30 min	59.00	–	67.60	3.30	–	0.87	1.10	2.10	0.04	0.05	–	1.00	–	11.40	–	0.86	
		450 °C 30 min	48.00	–	62.90	2.82	–	1.45	1.10	2.90	0.09	0.07	–	1.20	–	35.60	–	0.56	
		550 °C 30 min	38.00	–	63.60	1.72	–	1.39	0.52	2.30	0.16	0.05	–	0.64	–	14.61	–	0.16	
	Iron-bentonite	250 °C 30 min	76.00	–	48.70	5.15	–	0.50	0.73	1.20	0.01	0.05	–	0.35	–	15.91	–	0.88	
		350 °C 30 min	63.00	–	57.20	3.51	–	0.80	1.40	2.50	0.03	0.12	–	0.82	–	24.14	–	0.77	
		450 °C 30 min	42.00	–	61.00	2.79	–	0.84	1.30	2.50	0.03	0.12	–	0.63	–	56.87	–	0.73	
		550 °C 30 min	38.00	–	70.20	2.49	–	0.79	0.63	1.70	0.10	0.10	–	0.37	–	31.64	–	0.42	
Potato stem	Untreated	500 °C 6 h	14.89	10.40	75.81	–	19.30	–	–	–	0.39	1.51	–	–	1.49	24.67	99.43	0.08	
	Natural attapulgite	500 °C 6 h	30.71	9.93	59.75	–	30.92	–	–	–	1.15	2.13	–	–	2.05	50.33	90.4	0.12	
Bamboo	Untreated	600 °C 1 h	–	–	80.89	2.43	14.86	0.15	–	0.00	0.04	0.34	0.01	0.52	0.23	–	375.5	–	Yao et al.
Bagasse			–	–	76.45	2.93	18.32	0.79	–	0.05	0.11	0.91	–	0.15	0.21	–	388.3	–	[21]
Hickory chip			–	–	81.81	2.17	14.02	0.73	–	0.01	0.01	0.82		0.24	0.13	–	401.0	–	
Bamboo	Montmorillonite (MMT)	600 °C 1 h	–	–	83.27	2.26	12.41	0.25	–	0.23	0.68	0.21	0.14	0.33	0.14	–	408.1	–	
Bagasse			–	–	75.31	2.25	18.87	0.75	–	0.47	0.75	0.85	0.13	0.32	0.22	–	407.0	–	
Hickory chip			–	–	80.93	2.21	15.14	0.28	–	0.15	0.32	0.57	0.04	0.11	0.19	–	376.1	–	
Bamboo	Kaolinite (KLN)	600 °C 1 h	–	–	81.02	2.15	15.85	0.25	–	0.08	0.30	0.19	–	0.07	0.05	–	239.8	–	
Bagasse			–	–	70.20	2.44	24.44	0.74	–	0.46	0.53	0.88	–	0.06	0.16	–	328.6	–	
Hickory chip			–	–	78.08	2.11	18.12	0.33	–	0.07	0.51	0.52	–	0.05	0.18	–	224.5	–	
Bamboo	Untreated	400 °C 1 h	–	5.3	76.05	3.47	19.04	037	0.37	–	–	–	–	–	–	–	2.27	–	Chen et al.
	Montmorillonite	300 °C 1 h	70.00	6.60	–	–	–	–	–	–	–	–	–	–	–	–	9.84	0.05	[73]
		350 °C 1 h	64.00	6.90	–	–	–	–	–	–	–	–	–	–	–	–	13.40	0.05	
		400 °C 1 h	61.00	7.10	64.01	3.81	10.03	0.41	0.44	–	–	–	–	–	–	21.3	19.93	0.06	
		450 °C 1 h	58.30	7.40	–	–	–	–	–	–	–	–	–	–	–	–	26.22	0.06	
		500 °C 1 h	56.00	7.6	–	–	–	–	–	–	–	–	–	–	–	–	18.05	0.05	
Pine wood (PW)	Untreated	600 °C 1 h	–	–	85.70	2.10	11.4	0.30	–	0.02	0.04	0.19	–	0.05	0.12	–	209.60	–	Wang et al.
Bamboo	Natural Hematite		–	–	51.70	1.40	43.1	0.20	–	2.95	0.24	0.10	–	0.04	0.14	–	193.10	–	[87]
Corncob	Untreated	500 °C 2 h	–	8.74	82.84	2.11	–	1.36	–	–	–	–	–	–	–	16.21	16.50	–	Frišták et al.
	$Fe(NO_3)_3$		–	3.38	74.56	1.61	–	2.42	–	–	–	–	–	–	–	14.18	6.19	–	[74]
Pistachio shells (PI)	Untreated	400 °C 1 h	31.40	6.40	73.42	2.93	23.44	0.21								1.70	196.40		Komnitsas
	KOH		–	6.10	78.24	3.07	17.95	0.74	–	–	–	–	–	–	–	–	572.40	–	and Zaharaki
	$FeCl_3$		–	5.70	75.4	2.95	20.94	0.71	–	–	–	–	–	–	–	–	421.50	–	[88]
Pecan shells (PC)	Untreated	400 °C 1 h	34.70	6.10	71.6	2.65	25.15	0.6	–	–	–	–	–	–	–	1.80	142.40	–	
	KOH		–	5.80	75.3	2.75	21.09	0.76	–	–	–	–	–	–	–	–	397.30	–	
	$FeCl_3$		–	5.60	72.8	2.63	23.85	0.72	–	–	–	–	–	–	–	–	351.60	–	
Sawdust (SD)	Untreated	400 °C 1 h	17.70	4.80	65.2	2.08	32.4	0.32	–	–	–	–	–	–	–	1.70	48.7.0	–	
	KOH		–	4.60	72.9	2.19	24.52	0.39	–	–	–	–	–	–	–	–	124.60	–	
	$FeCl_3$		–	4.40	67.3	2.11	30.23	0.36	–	–	–	–	–	–	–	–	110.80	–	
Wheat straw	Untreated	600 °C 1 h	27.90	6.90	–		–	–	–	–	–	–	–	–	–	–	4.50	0.01	Tang et al.
	Graphene (G)0.1%		25.70	6.40	–	–	–	–	–	–	–	–	–	–	–	–	10.90	0.03	[79]
	G- 0.5%		27.70	6.70	–	–	–	–	–	–	–	–	–	–	–	–	15.80	0.06	
	G − 1.0%		29.00	7.10	–	–	–	–	–	–	–	–	–	–	–	–	17.30	0.12	
Paper and paper sludge	Untreated	750 °C 2 h	–	8.46	–	–	–	–	–	0.30	–	–	–	–	–	36.20	174.00	40.00	Chaukura
	Fe_2O_3		–	2.86	–	–	–	–	–	22.60	–	–	–	–	–	49.30	15.30	3.50	et al. [75]

samples due to the thermal stability of metal oxide and clay minerals [73,75,83].

A slight decrease in the C content of BC composites resulting from metal and clay modification [74,83] may occur due to the introduction of metallic elements. For instance, some elements in modifiers may play a role of a catalyst that results in the different contaminant degradation mechanisms. However, feedstock and temperature are the main factors determining C content. At high pyrolysis temperature, C content increases [52] due to high carbonization and dehydrogenation, and a high amount of C exists within aromatic structures [85]. High C content in the feedstock produces BC composites with higher C contents due to the insufficient amount of hydrogen in its structural matrix [86].

The pH of the BC composite can be varied according to the acidity or basicity of the combining material as well as the pyrolysis temperature [75,89]. Depending on the level of O in the clay minerals, clay modification of BC can alter the O content and may introduce additional oxygen-containing functional groups to the BC surface [83]. However, chemical modification results in slight decrease in the H, O, and N contents [88]. Furthermore, surface functional groups determine the surface acidity/basicity, which is a crucial factor affecting the adsorption capacities and selectivity of clay–BC composites. Most of the clay minerals used in BC composites mainly consist of metals such as Ca, Na, Al, Mg, Fe, Zn, and Si [90]. As such, metal concentrations are higher in clay BC composites than in pristine BC [21,77,83].

The electrical conductivity (EC) of BC significantly increases when it is pyrolyzed at high temperatures [43,48,83], due to the loss of volatile material at high temperatures and the different crystalline structural matrix of C. Modification with metal oxides increases the soluble salt content within composites, thus increasing the EC of BC composites [75]. However, modification with metals otherwise reduces the EC of modified BC [74].

Clay-modified BC exhibits comparable thermal stability to that of unmodified BC [21]. Conversely, BCs modified using carbonaceous materials exhibit higher thermal stability than unmodified BC [78,79]. If the modifying agent has magnetic properties, the composite may exhibit permanent magnetic properties after pyrolysis [78].

Upon chemical modification, the surface of BC becomes rough as a result of adherence of fine particles of the modifier [77]. Scanning electron microscopy (SEM) allows the clear visualization of fine particles adhered on BC surfaces [74,79,83], which mostly act to increase surface area as well as adsorption capacity. However, the surface area can be decreased if pores are clogged as a result of excessive coating [74]. Increases in pyrolysis temperature and residence time also increase specific surface area, pore volume, and pore size of BCs due to the thermal destruction of H and oxygen-containing functional groups including aliphatic alkyl, ester, and phenolic groups.

5. Sorptive removal of inorganic contaminants by biochar composites

5.1. Nutrients

The release of nutrients such as nitrate, ammonia, and phosphate to the natural ecosystem increases the level of growth-limiting nutrients in natural water bodies, and promotes the growth of photosynthetic organisms, which can ultimately lead to eutrophication of aquatic ecosystems. Although phosphate can be removed by many adsorbents, the parallel process for nitrate is rather difficult. However, BC is able to remove phosphate, nitrates, and ammonium from aqueous media [91]. In some instances, BC is unable to remove nitrate, and some BC itself releases nitrate and phosphate into the solution [48]. At high pH values, phosphate adsorption capacity decreases because the surface of BC is negatively charged.

Nevertheless, compared to raw BC, modified BCs have demonstrated high potential in removing nutrients from aquatic systems. Table 4 summarizes the applications of modified BCs in the removal of contaminants present in water. In some cases, modifications of BC can cause differential adsorption effects for the same contaminant, possibly due to the influence of feedstocks [23]. The SBT-BC has shown a very low phosphate removal rate (approximately 10%) [91] compared to SBT-MgO-BC (66.7%), which is explained by the strong affinity of MgO for phosphate in aqueous medium due to its high general affinity for anions through mono-, bi-, and tri-nuclear complexation [92]. However, the complexation mechanism depends on the amount and distribution of MgO particles on the BC surface as well as the size of MgO particles. Interestingly, PW-MgO-BC achieved a much lower phosphate removal rate (0.5%) [23]. Electrostatic repulsions between the BC surface and phosphate in solution was the reason for the low adsorption of phosphate by PW-MgO-BC [93]. Nitrate removal by PS-MgO-BC and SBT-MgO-BC was found to be 11.7% and 3.6%, respectively [23], which might be due to differences in the adsorption mechanisms involved.

Chitosan-modified BC had not achieved promising results in the removal of phosphate from solution because of net negative charge of the modified BC surface [78]. In contrast, zerovalent iron (ZVI)-modified BC removed high concentrations of phosphate, and removal efficiency was found to increase from 56% with increasing amount of Fe. The pH of the medium (5.7) was lower than the pH_{pzc} (7.7) of ZVI, and thus, the cationic form predominantly existing in this solution might have promoted the binding of phosphate [94].

The enhanced adsorption capacities exhibited by BB-MMT-BC composite for ammonium and phosphate were due to enhanced surface area of BC and increased number of binding sites resulted from the clay modification [73]. Adsorption of phosphate and ammonium on the BB-MMT-BC composite at low concentrations was mainly controlled by monolayer adsorption (chemical adsorption), while at higher concentrations both chemical and physical adsorption were involved, although multilayer adsorption also played an important role [73].

5.2. Trace metals

Presence of elevated trace metals concentrations in natural ecosystem potentially leads to severe environmental concerns [37]. Most commonly found trace metals in aquatic ecosystem are Pb, Hg, Cr, As, Cd, Zn and Cu. The United States Environmental Protection Agency (EPA) has set the maximum allowable limit of above metals in drinking water and waste water. Therefore, various methods were developed, such as chemical precipitation, reverse osmosis, ion exchange, solvent extraction, electro-dialysis and adsorption for removing trace metals from contaminated water. Due to relative expensiveness adsorption is considered as economically feasible method for the removal of trace metals from aqueous media (Table 4).

The adsorption capacities of bentonite–BC composites for Cr(VI) and Zn(II) were lower than that was achieved with raw BC and bentonite [22], and it was suggested that the binding of anionic functional groups of the BC with the cationic compounds of the bentonite (and vice versa) may have reduce the available adsorption sites.

The adsorption of As(V) onto the hematite-modified BC was roughly double than that of the pristine BC at all concentrations, further suggesting that iron oxide particles served as adsorption sites with a higher affinity than the unmodified BC for As in aqueous solution [87]. The adsorption of As(V) onto a solid surface is mainly controlled by As speciation and the charge of the sorbent surface [95].

Among three BC composites prepared by combining with different weight percentages of Mn, the highest adsorption efficiency for Pb(II) (98.9%) was shown by BC composite loaded with 3.65% Mn. However, BC composite coated with excessively high amount of Mn exhibited low Pb(II) adsorption efficiency because of coating leading to reduction of surface area via blockage of pores [77]. Solution pH influenced both Pb (II) species and net surface charges on the BC composite, which directly influenced Pb(II) adsorption [77].

Removal of mercury increased with an increase in G content from 0.1 to 1.0% in a WS-G–BC composite [79]. The removal of Hg was

Table 4
Applications of modified BCs for the removal of toxic contaminants in water.

Feedstock	Modifier	Pyrolysis Conditions	Contaminant	Enhancement	Mechanism	Reference
Potato stem	Natural attapulgite	500 °C 6 h	Norfloxacin	Maximum adsorption capacity was 1.7 times higher than raw PSt-BC. More than 80.1% of NOR was removed in a wide range of pH values (2.0–11.0).	The SiO_2 particles and oxygen-containing surface functional groups serve as sorption sites for adsorption. Electrostatic interaction is the main mechanism involved.	Li et al. [83]
Sweet sorghum bagasse (SSB)	Bentonite	400 °C 1 h	Malachite green (MG)	MG adsorption capacity of the composite was higher than that of pristine BC.	Net negative charge of the BC-composite is improved the attraction of cationic dyes via electrostatic interactions.	Fosso-Kankeu et al. [97]
Bamboo Bagasse Hickory chip	Montmorillonite	600 °C 1 h	Methylene blue (MB)	The MB removal rate of BG–MMT-BC and HC–MMT-BC composites has been improved compared to raw BCs but decrease the MB adsorption capacity of BB–MMT-BC composite than raw BC.	The superior ion-exchange capacity of MMT clay improved the adsorption capacity of BC composites.	Yao et al. [21]
Bamboo Bagasse Hickory chip	Kaolinite	600 °C 1 h	MB	The MB removal rate of BG-KLN-BC and HC-KLN-BC was slightly improved compared to raw BCs and removal rate of MB by BB-KLN-BC decreased compared to raw BC.		
Sweet sorghum bagasse	Bentonite	400 °C	Zn(II)	Adsorption capacity of the composite was lower for Zn(II) compared to bentonite and raw BC.	The anionic functional groups on the BC that partially bind with the cationic compounds in bentonite and obstruct pores.	Fosso-Kankeu et al. [22]
			Cr(VI)	Adsorption capacity of Cr(VI) by composite is higher than bentonite and slightly higher than raw BC.		
Pine wood	Natural Hematite	600 °C 1 h	As(V)	These γ-Fe_2O_3 particles act as sorption sites for As(V) and increase adsorption capacity of As(V).	BC Composite has exhibited magnetic properties due to conversion of natural hematite into γ-Fe_2O_3 particles with magnetic properties. Electrostatic interactions involved in adsorption.	Wang et al. [87]
Bamboo	Montmorillonite	400 °C 1 h	Phosphate Ammonium	Adsorption capacity for phosphate is 8.4 times higher than ammonium.	Adsorption of P was resulted via electrostatic attraction or ionic bonds between P and cations in the BC composite. The adsorption of ammonium was occurred via surface adsorption onto the MMT, BC and intercalation into the gallery of MMT.	Chen et al. [73]
Bamboo	Zerovalent iron	600 °C 1 h	MB	Among all the iron-modified BCs, the BC composite with the highest weight ratio of Fe (3 times of BC mass) achieved the highest MB removal rate.		Zhou et al. [78]
			Pb(II)	More than 93% of Pb(II) was removed.	The ZVI can remove heavy metal cations; Pb(II), Cr(VI) and As(V) from aqueous solution through both adsorption and reduction processes. Electrostatic attractions between the anions and the ZVI particles on the composite surface.	
			Cr(VI)	The removal of Cr(VI) increased with the amount of ZVI in the samples when the mass ratios of the other components were constant.		
			As(V)	Removal rate of As(V) by BB-ZVI-BC composite increased from 72%.		
			Phosphate	Phosphate removal increased from 56%.		
Rice husk (RH)	Ca^{2+}	300 °C 1 h 17 °C min^{-1}	As(V)	Percentage removal of As(V) increased from about 70% compared to raw BC.	Due to alkaline nature of solution calcium oxide removed As via precipitation.	Agrafioti et al. [98]
			Cr(VI)	Percentage removal of Cr (VI) slightly increased with modification.	High pH of BC composite solutions deprotonate their functional groups and repel negatively charged Cr(VI).	
Rice husk Solid waste	Fe^0	300 °C 1 h 17 °C min^{-1}	As(V)	Percentage removal of As(V) significantly increased with the modification and with the increase of percentage amount of Fe^0 removal percentage further increased. Percentage removal of As(V) from 40% and not changed with the percentage amount of Fe^0 available in BC composite.	The close to neutral nature and alkaline nature of their arsenic solutions respectively, indicated that As(V) was possibly removed by co-precipitation when $Fe(OH)_3$ was formed.	Agrafioti et al. [98]
			Cr(VI)	Percentage removal of Cr(VI) was slightly increased when the percentage amount of Fe^0 in composite high. Percentage removal of Cr(VI) was significantly decreased	High pH of RH-Fe^0 and SW-Fe^0 BC composite solutions deprotonate their functional groups and repel negatively charged Cr(VI).	

(*continued on next page*)

Table 4 (*continued*)

Feedstock	Modifier	Pyrolysis Conditions	Contaminant	Enhancement	Mechanism	Reference
				with the modification and further increase of percentage amount of Fe^0 in BC composite further decreased percentage removal.		
Rice husk Solid waste	Fe^{3+}	300 °C 1 h 17 °C min^{-1}	As(V)	Percentage removal of As(V) by RH-Fe^{3+} composite increased from 47% compared to raw BC and it further increase with the Fe^{3+} amount in composite Percentage removal of As(V) by SW-Fe^{3+} increased from about 40%, but it was not depend on percentage amount of Fe^{3+} in BC composite.	Highly acidic nature of solution promotes electrostatic interactions between positively charged BC surface and negatively charged As(V) species.	Agrafioti et al. [98]
			Cr(VI)	Percentage removal of Cr(VI) by RH-Fe^{3+} composite increased with the decrease of Fe^{3+} amount in the composite. Percentage removal of Cr(VI) was high when percentage amount of Fe^{3+} in BC composite is high.	Strongly acidic conditions cause an impact on the solubility of Fe^{3+} and which is negatively affected Cr(VI) adsorption on BCs.	
Reed straw	TiO_2	500 °C 6 h	Sulfamethoxazole (SMX)	As an adsorbent, the removal efficiency was less than that of unmodified BC. As a photocatalyst, degradation of SMX was higher than that of TiO_2.	The composite TiO_2-BC structure strengthened the photocatalytic activity of TiO_2.	Zhang et al. [99]
Pine wood	MnO_2	100 °C 1 h, then 700 °C 3 h	Pb	Biochar impregnated with 3.65% Mn exhibited the highest Pb(II) adsorption efficiency (98.9%).	High hydroxyl group density resulted in a lower pH_{pzc} value, which favored the removal of Pb(II).	Wang et al. [77]
Corncob	$Fe(NO_3)_3$	500 °C 2 h	Eu	Modification has no significant impact on adsorption of Eu.	Adsorption mainly occurred via chemisorption	Frišták et al. [74]
			As	Modified BC exhibit more than 20 times increase of adsorption for As compared to raw BC.		
Sugar beet tailings	MgO	600 °C 1 h	Phosphate and nitrate	Phosphate removal rate was 66.7%. Nitrate removal rate was 3.6%. Nitrate removal rate was 11.7%.	MgO has strong affinity for phosphate in aqueous medium due to its high general affinity for anions through mono-, bi-, and tri-nuclear complexation. However, the complexation mechanism depends on the amount and distribution of MgO particles on the BC surface as well as the size of MgO particles.	Zhang et al. [23]
Peanut shell Cottonwoods (CW)				Phosphate removal rate was approximately 40%. Nitrate removal rate was approximately 5.0%.		
Pine wood				Phosphate removal rate was 0.5%. Nitrate removal rate was approximately 5.0%.	Electrostatic repulsions between the BC surface and phosphate in solution results low adsorption of phosphate by PW-MgO-BC.	
Wheat straw	Graphene	600 °C 1 h	Phenanthrene, mercury	Removal efficiency of phenanthrene and mercury increased with the increase in G from 0.1 to 1.0%.	Modified BC surface exhibited more oxygen-containing functional groups and was negatively charged, which improved adsorption of phenanthrene and mercury.	Tang et al. [79]
Bamboo	Chitosan	600 °C 1 h	Pb(II),	Removal of Pb(II) enhanced from 35.7% relative to unmodified BC.	Amine functional groups of the chitosan have strong affiliation to cationic metal ions in aqueous solution.	Zhou et al. [78]
			Cr(VI)	Removal of Cr(VI) enhanced from 27.8%, compared to unmodified BC.		
			As(V) Phosphate MB	Did not remove anionic As(V) or phosphate from solution. MB removal rate was also high.	Surface of both raw BC and chitosan modified BC negatively charged.	
Sweet gum wood	Graphene oxide (GO) Carbon nanotubes	600 °C 1 h	Pb(II), Cd(II)	Adsorption capacities for Pb(II) and Cd(II) were higher than those of pristine BC. The GO–BC composite showed higher adsorption of Pb(II) and Cd(II) than the CNT–BC composite.		Liu et al. [82]

facilitated by the large surface area, allowing surface complexation between Hg and the increased oxygen-containing functional groups (−OH, O═C−O) and C═C groups on the surface of the composite containing 1% G [96].

In novel adsorbents prepared by combining BC with chitosan and ZVI, chitosan acted as a dispersing and soldering agent to attach ZVI particles to the BC surface [78]. Chitosan-modified BC increased the removal of Pb(II) compared to the unmodified BC because the amine functional groups of chitosan had strong affinities to cationic metal ions in the aqueous solution [81]. The presence of both ZVI and chitosan increased the removal of Pb(II) up to 93%, which is exempted from the amount of ZVI present in the composite. However, removal of Cr(VI) increased with an increasing amount of ZVI in the composite; the highest removal rates observed were 35 and 40% (for BB:chitosan:ZVI 1:1:3 and 1:2:3, respectively), indicating that both chitosan and ZVI particles conferred enhancement to the removal of cationic heavy metals [78]. Unmodified BC and chitosan-modified BC did not achieve significant removal of anionic As(V) from solution [78], which might have been due to their surfaces having net negative charges [81]. However, ZVI-modified BC removed between 23 and 95% of As(V), and increasing the Fe level in the composite further improved removal of As (V). The pH_{pzc} of ZVI is reported around 7.7 [94]. As the pH of the medium (5.7) was lower than the pH_{pzc}, ZVI particles were positively charged and could have assisted the adsorption of the anionic As(V).

Both Ca and Fe modified BCs exhibited high As(V) removal capacities (95%), except for that produced using a RH feedstock impregnated with Fe^0, which removed only 58%. However, the Cr(VI) removal rate was not as high as expected; the highest removal rate (95%) was achieved by RH-BC impregnated with Fe^{3+} [98].

Engineered BCs (EBC) produced using stillage residue collected from a biofuel pilot plant, which manufactures ethanol, were used for the removal of Ag(I) from an aqueous medium. The removal percentage of Ag(I) reached 97.4%. Adsorption of Ag(I) on EBC occurred via multilayer sorption, and that the process could be governed by multiple mechanisms [100].

Both GO–BC and CNT–BC composites prepared from sweet gum feedstock achieved higher adsorption capacities for Pb(II) and Cd(II) than the pristine BC. The GO–BC composite exhibited higher adsorption of Pb(II) and Cd(II) than the CNT–BC composite [82]. Adsorption of both metals could be governed via complexation with oxygen-containing functional groups of the carbon nano-materials, electrostatic attractions, cation exchange, and surface adsorption onto the CNTs, GO, and BC surfaces [101].

Pine bark waste was impregnated with $CoFe_2O_4$ has shown low removal percentage for both Pb(II) and Cd(II), and removal was clearly pH-dependent, and removal percentage increased with increase of pH from 2.0 to 8.0. At acidic pH due to the presence of high concentration of H^+ on the BC composite, BC surface was protonated and became positively charged. It therefore reduced the adsorption of metal ions due to electrostatic repulsion. At high pH, BC composite surface charged negatively, thus adsorption of metal ions increased.

The Cu(II) adsorption capacity of nano MnO_2 BC composite enhanced with the increase of pH between 3.0 and 6.0, and comparatively higher than that of nano MnO_2. Formation of complexes between Cu(II) and oxygen-containing functional groups present on BC composite surface was the major mechanism involved in the metal adsorption [102].

Magnetic BC prepared via impregnating with different mass ratios of $FeSO_4$ and $NaBH_4$ was showed affinity for Cu(II), and the adsorption affinity increased with the increase of molar ratio of $FeSO_4$ and $NaBH_4$ in the BC composite. Sorption capacity increased with the long stirring time, and decreased with the higher initial concentration of Cu(II) in the solution. Main functional groups contributing to the coordination of Cu(II) on the BC surface were carboxyl, hydroxyl and phenolic groups. Partial deprotonation of the functional groups under acidic conditions promoted the adsorption of Cu(II) via exchanging Cu(II) with hydrogen ions [103].

Hydrogel BC composite was synthesized by embedding RH-BC into poly(acrylamide) hydrogel with N.N'-methylenebisacrylamide (MBA) as cross linker. Removal of As increased with the increase of pH from 4.0 − 6.0, and decreased beyond pH 6.0–10.0. High As adsorption at pH 6.0 facilitated by electrostatic interactions occurred between oxyanion species of As and positively charged BC surface because at $pH < pH_{PZC}$ due to protonation of surface-active sites BC surface became positively charged. At $pH > pH_{PZC}$, BC surface was negatively charged, and decreased the adsorption of As due to repulsive effect. Alternatively, increase of hydroxyl ions in the solution competing with As species reduced the adsorption of As at high pH [104].

Higher removal efficiency of Pb(II) was demonstrated by magnetic ZnS-BC composite compared to magnetic BC, however it was pH dependent and beyond pH 6.0 Pb(II) precipitated as hydroxide [105]. The adsorption of Pb(II) was suggested as an endothermic and spontaneous process. In a different study, adsorption of Pb(II) by MgO-BC composite was reported to be rapid, and reached 99.9% within 10 min. Adsorption capacities remained constant at the pH range of 3.0 to 7.0 dominated by ion-exchange between Pb^{2+} and Mg^{2+} [106].

6. Sorptive removal of organic contaminants

The main organic contaminants in aqueous bodies are pesticides, pharmaceuticals, antibiotics, and polycyclic aromatic hydrocarbons. For the adsorption of organic contaminants, modified BC has been widely used. Attapulgite–BC composites derived from lotus stalk biomass and natural attapulgite adsorbed more than 80.1% of NOR from aqueous solution over a wide range of pH values (2.0–11.0), because pH had a major impact on the molecular form of NOR, and the surface charge of the BCs [107]. The removal capacity of NOR by the composite was very high compared to that of the unmodified BC. This might be due to the high adsorption capacity of attapulgite particles for NOR [83].

Acid pretreated titanium dioxide (TiO_2)-reed straw BC (TiO_2-pBC) and acid pretreated reed straw BC (pBC) were produced via a sol-gel method [99]. TiO_2 particles covered the surface and filled internal pores of the pBC, reducing the surface area of the adsorbent. Thus, the adsorption capacity of TiO_2-pBC produced at 300 °C for SMX was lower than that of pBC. The degradation of SMX was significantly higher by TiO_2-pBC produced at 300 °C compared to its degradation under simulated sunlight and UV light. Furthermore, the SMX degradation efficiency of TiO_2-pBC produced at 300 °C reached 91.27%, which was much higher than that achieved with pure TiO_2 (58.4%). Therefore, the composite TiO_2-pBC structure strengthened the photocatalytic activity of TiO_2 [108].

Liquid phase reduction method was used for the production of BC composite (Co/Fe/MB) under anaerobic conditions. The BC composite was shown the highest cefotaxime removal efficiency of 82.48% and it decreased slightly with increased pH from 4.0 to 9.0, but significantly decreased at neutral and alkaline conditions [109]. Electrostatic attraction supported the adsorption because of that the surface of composites was positively charged below pH 6.0. The catalysis of produced atomic hydrogen further enhanced the removal efficiency of cefotaxime (CFX). Nevertheless, the CFX removal efficiencies were equal at pH 4.0 and 5.0, which indicated that the hydrogen ion concentration was still enough for the formation of atomic hydrogen at pH 5. The CFX removal efficiency decreased significantly with the increase of pH (alkaline and neutral conditions) as a result of passivation of layers and less atomic hydrogen production on the surface of Co/Fe/MB [110,111].

Phenanthrene removal efficiency increased from 63.3 to 94.9% with an increase of G percentage of BC from 0 to 1%. Adsorption occurred via partitioning, π–π interaction, surface adsorption, pore-filling, and electrostatic attractions [48]. The coating of G on the surface of BC resulted in greater surface area, pore size, pore volume, stronger vibration of C═C bonds, an increasing negative surface charge, and more

oxygen-containing groups. Therefore, G-modified BC more effectively removed phenanthrene than raw WS-BC (Table 4).

Raw BG-BC, BB-BC, and HC-BC all demonstrated very low MB removal rates. Upon surface modification with MMT and KLN, MB adsorption capacities increased. However, such modification slightly reduced the removal of MB by the BB-MMT-BC and BB-KLN-BC, possibly due to obstruction of pores by clay particles [21]. (Table 4).

Chitosan– and ZVI–BC composites achieved higher removal of MB from aqueous solution than unmodified BC. Among all the iron-modified BCs, the BC composite with the highest amount of Fe achieved the highest MB removal rate. This enhanced removal can be due to both surface adsorption and chemical reduction mechanisms [112].

The adsorption efficiency of MO by ZVI-modified RH-BC was studied in composites prepared with ZVI:BC ratios of 1:3, 1:5, and 1:7. The highest MO adsorption efficiency for ZVI–BC composites was shown at 1:5 ratio (98.5%), and further increase of ratio to 1:7 slightly decreased the MO adsorption efficiency (95.2%) [113]. The MO is an anionic dye, and its adsorption was favored by the positively charged ZVI particles, as its pH_{pzc} was 8.0, which was higher than the pH of the solution (5.6) [94].

Magnetic BC and activated BC were prepared using tannin BC and exhausted husk obtained by black wattle. The adsorption capacities of activated BC and magnetic BC for thiacloprid (TCL) and thiamethoxam (TMX) were 1.02, 0.97 mg g^{-1} and 0.73, 0.40 mg g^{-1}, respectively. Adsorption of pesticides on to activated BC mainly occurred via π–π EDA interactions due to the presence of aromatic rings in BC, while magnetic BC had more polar groups (−OH).

7. Factors influencing adsorption

The factors governing the adsorption rate are the BC's surface area, nature and initial concentrations of adsorbate, solution pH, temperature, interfering substances, properties and amount of adsorbent. Adsorption is proportional to the surface area available for adsorption in general however, the magnitude differs [114]. Hence, materials with more pores and higher surface area usually increase adsorption due to the enhanced mass transferring mechanisms, however, this depends on various other factors such as chemical composition of the adsorbate, size and its speciation. In case of a composite preparation, excess coating of a material may leads to obstruction of pores, resulting in significant decrease in the pore volume, and hence it reduces the adsorption capacity [22]. This was apparent in excessive hydrous manganese oxide incorporated BC [77].

The physicochemical nature of the adsorbent strongly impacts on adsorption rate and adsorption capacity. Fine powder adsorbents have higher adsorption capacity than those consisting of large particles due to the increase in surface area [115]. The presence of surface functional groups promotes chemical interactions, and thus the adsorption capacity can be enhanced by increasing the concentration of appropriate functional groups, however, this may influence negatively based on the composition of the functional group. The presence of cations or anions on the surface of the adsorbent may enhance its ion-exchange capacity, which is an important mechanism in the removal of heavy metals.

Adsorption occurs within pores of the adsorbent, so molecular size of the adsorbate is also related to adsorption rate and capacity. If the rate is controlled by intra-particle transport, adsorption rate will increase with decreasing molecular weight of the adsorbate molecules [116].

Further, pH has a major impact on the adsorption process as it directly influences both the chemical form of the contaminant and the surface charge as well as ionization or speciation of the adsorbate [83]. Incorporation of a material in preparation of a composite may influence the change in pH_{pzc} [72].

Adsorption reactions are exothermic reactions; thus adsorption, is temperature dependent, typically increases with increasing temperature. Furthermore, adsorption may be influenced positively or negatively by the presence of interfering organic or inorganic compounds. At the same time, the presence of natural organic matter may impact on adsorption which could be positive or negative depending on the adsorbate properties. A study reported the influence of cadmium ions (Cd^{2+}) on the adsorption of SMX by Cd^{2+} neutralizing the surface of BC [117]. Competitive adsorption between different chemicals generally occurs at the solid–water interface and can generate an impact to the sorption characteristics and affinity of the adsorbent for each contaminant. The presence of oxytetracycline (OTC) significantly inhibits the adsorption of carbaryl (CBL) on the original BC (produced at 600 and 700 °C) indicating a competing effect between OTC and CBL adsorption [56].

8. Mechanisms involved

Several mechanisms are responsible for the removal of contaminants from aqueous solutions using BCs and modified BCs, including electrostatic interactions, ion-exchange, hydrogen bonding, surface complexation, pore-filling mechanisms and π–π EDA interactions may occur simultaneously [118]. Fig. 3 illustrates the major mechanisms involved in adsorption of contaminants on modified BC.

The surface of BC composites can be positively or negatively charged depending on the pH of the medium. When pH is higher than pH_{pzc}, the surface of the adsorbent is negatively charged, and when pH is lower than $pH_{pzc,}$ the surface is positively charged [119]. This can facilitate electrostatic attraction between the BC surface and the cationic or anionic forms of contaminants. Such electrostatic attractions have been reported in many studies i.e. on the adsorption of NOR by PSt-attapulgite–BC composite [83], adsorption of phosphate by a BB-MMT–BC composite produced at 400 °C [73], and adsorption of As by a magnetic BC composite prepared from PW and natural hematite [87]. Positively charged metal ions attached to the BC surface also encourage adsorption of anionic compounds via electrostatic interactions [73], and can further promote adsorption of metals via ion-exchange mechanisms [19] Adsorption via ion-exchange mainly depend upon the size of metal and the available functional groups on the BC surface [37]. Also the presence of a clay mineral with a high ion-exchange capacity on the BC surface stimulates adsorption of contaminants such as organic dyes and antibiotics via ion-exchange mechanisms [21]. In additional contaminants can exchange with ions available in the interlayer spaces of combined clays, which is referred as intercalation interactions [66].

The presence of oxygen-containing functional groups promotes adsorption of toxic organic compounds via hydrogen bonding and complexation between BC and the contaminant [107]. Meanwhile, cationic metals and anionic metals/metalloids can be bound by these oxygenated functional groups via electrostatic attraction [19]. However, the presence of a large number of functional groups and mineral components on the surface can negatively affect this adsorption mechanism by blocking the trajectories to pores on the BC surface [25,120].

The porous structure of BC surfaces facilitates adsorption of organic compounds via a pore-filling mechanism [51]. During modification, the deposition of modifying materials on the BC increases the surface area of BC, thereby enhancing the number of adsorbates which can be adsorbed on the surface [83].

In some cases, adsorption is based on physical bonding/intermolecular forces such as *van der Waals* and dipole-dipole interactions. Ammonium adsorption onto BB-MMT–BC composite produced at 400 °C was suggested to be primarily controlled by *van der Waals* forces and to a lesser extent by a cation-exchange process [73].

Adsorption of organic pollutants can be further governed by π–π EDA interactions between BC and aromatic groups of organic compounds. Removal efficiency of phenanthrene is dominated by π–π EDA interactions as well as surface adsorption, partitioning, and electrostatic attractions [79]. Mostly, adsorption of trace metals occurs via surface complexation mechanism, i.e., via diffuse double layers. Mercury adsorption occurs via surface complexation between mercury and the

oxygen-containing functional groups (−OH, O═C−O) and alkene (C═C) groups on the surface of a BC composite containing 1% Graphene [96].

9. Future perspectives

This review highlighted the utilization of engineered BC for the management and removal of frequently encountered inorganic and organic pollutants in the aquatic systems. Modification tailors surface properties of BC (surface area, pore volume, pore size, surface charge, and surface functional groups). A range of modifiers has been used combining with BC, such as clays, metals, metal oxides, zero-valent ion and organic compounds (polymer, graphene, graphene oxide). Overall, the modifying agents exert promising improvement in adsorption capacities, but sometimes show negative effects on the adsorption capacity of target contaminants. Hence, further investigations require to identify compatible modifiers for targeting specific contaminants. It can be done via changing the nature of adsorbents including the physical and chemical properties. Environmental conditions can also be altered to improve the adsorption efficiency including maintaining temperature and pressure. In addition, high-end instruments such as HPLC and ICP can be used to achieve high detection limit of contaminants.

Among modified BCs, role of clay–BC composites as adsorbents in waste water remediation has not been extensively studied. Nevertheless, the limited published data offer adequate proof for the effectiveness of clay–BC composites as adsorbents for the removal of nutrients, metals and dyes. Even though surface area is often reduced due to blockage of pores, the combined effect of BC and clay minerals improves the adsorption capacity of clay–BC composites significantly, especially when layered clays are combined with BC. Hence, further studies will be essential to enhance the knowledge regarding surface chemistry, adsorption mechanisms and the factors influencing the adsorption capacities of clay–BC composites prepared by clay minerals. Furthermore, employing waste clay materials such as red mud and steel slag with biochar application can be a desirable end use.

Modification of BC with metals or metal oxides has been studied in relation to several contaminants. Certain modifiers negatively impacted the adsorption of a given contaminant, justifying further investigation. Neither pristine BC nor BC composites have been demonstrated to improve adsorption of nutrients (phosphates and nitrates) which are the main compounds responsible for polluting fresh water ecosystems and causing eutrophication. Thus, further research is necessary to develop or identify a suitable adsorbent for the control of these nutrients.

Recently, functionalized biochar has been successfully applied for various applications. Functionalization process of biochar allows tuning of its surface properties and functionality [26], hence can be applied for various sustainable processes. Design of functionalized biochar based composites is suggested in order to further enhance performance of different applications.

Most adsorption studies were conducted under laboratory conditions. However, the natural environment often differs significantly from the laboratory environment, especially concerning continuous fluctuations in pH and temperature, each of which exert substantial influence on the adsorption of most adsorbents studied. Hence, pilot-scale testing will be essential for determining the stability and efficacy of BCs and their composites in environmental remediation. Furthermore, long-term investigations are mandatory to assess the stability of BC composites and ensure their environmental friendliness. In addition, information regarding large-scale production of engineered BC is limited and should be documented. A production cost analysis is another key undertaking that will allow the estimation regarding the profitability of BC-based remediation compared to other techniques available. The increasing quantity of municipal solid waste can be combined with naturally abundant clay materials via simple pyrolysis process to make clay-BC composites. Bio-oil and gases produced during the pyrolysis process can be utilized for the energy production.

In recent decades, the environment has been exposed to a diverse group of emerging contaminants such as pharmaceuticals, personal care products, endocrine disrupters, hormones, and toxins, owing to rapid industrialization and anthropogenic activities. Because BC composites have been used as adsorbents for the elimination of both organic and inorganic contaminants, they should be considered as candidate materials for use in efforts to mitigate the spread and effects of such emerging contaminants.

Other than adsorption, removal of contaminants via degradation using metal oxide BC composite was achieved. Therefore, the BC composites showed evidence of strengthening the photocatalytic activity of catalysts. Thus, future research should focus on the generation

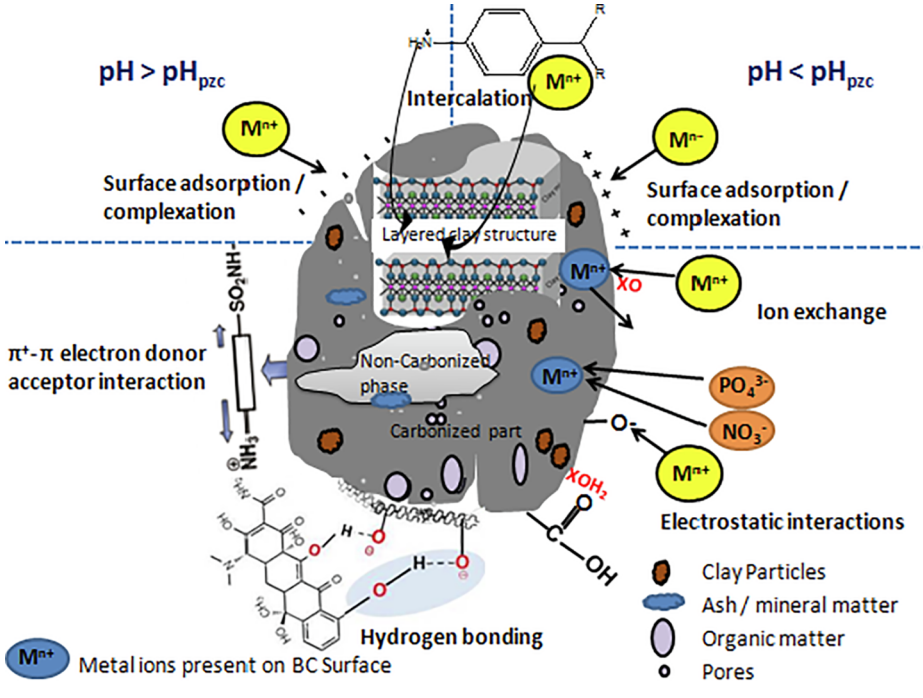

Fig. 3. Possible mechanisms of adsorption of inorganic and organic compounds on modified biochar.

of engineered BCs, which can be used for complete and long-term removal of emerging contaminants.

Acknowledgement

Financial support from the grant ASP/01/RE/SCI/2017/83 from the Research Council, University of Sri Jayewardenepura is acknowledged.

Appendix A. Supplementary data

Supplementary data to this article can be found online at https://doi.org/10.1016/j.cej.2019.04.097.

References

[1] J. Lehmann, S. Joseph, Biochar for Environmental Management: Science and Technology, Earthscan, UK, 2009.

[2] J.S. Cha, S.H. Park, S.-C. Jung, C. Ryu, J.-K. Jeon, M.-C. Shin, Y.-K. Park, Production and utilization of biochar: a review, J. Ind. Eng. Chem. 40 (2016) 1–15.

[3] K. Qian, A. Kumar, H. Zhang, D. Bellmer, R. Huhnke, Recent advances in utilization of biochar, Renew. Sustain. Energy Rev. 42 (2015) 1055–1064.

[4] J. Lee, K.-H. Kim, E.E. Kwon, Biochar as a catalyst, Renew. Sustain. Energy Rev. 77 (2017) 70–79.

[5] M. Ahmad, A.U. Rajapaksha, J.E. Lim, M. Zhang, N. Bolan, D. Mohan, M. Vithanage, S.S. Lee, Y.S. Ok, Biochar as a sorbent for contaminant management in soil and water: a review, Chemosphere 99 (2014) 19–33.

[6] Y. Yao, B. Gao, M. Zhang, M. Inyang, A.R. Zimmerman, Effect of biochar amendment on sorption and leaching of nitrate, ammonium, and phosphate in a sandy soil, Chemosphere 89 (2012) 1467–1471.

[7] Z. Shen, Y. Zhang, O. McMillan, F. Jin, A. Al-Tabbaa, Characteristics and mechanisms of nickel adsorption on biochars produced from wheat straw pellets and rice husk, Environ. Sci. Pollut. Res. 24 (2017) 12809–12819.

[8] M. Vithanage, S.S. Mayakaduwa, I. Herath, Y.S. Ok, D. Mohan, Kinetics, thermodynamics and mechanistic studies of carbofuran removal using biochars from tea waste and rice husks, Chemosphere 150 (2016) 781–789.

[9] I. Herath, P. Kumarathilaka, M.I. Al-Wabel, A. Abduljabbar, M. Ahmad, A.R.A. Usman, M. Vithanage, Mechanistic modeling of glyphosate interaction with rice husk derived engineered biochar, Microporous Mesoporous Mater. 225 (2016) 280–288.

[10] S.S. Mayakaduwa, P. Kumarathilaka, I. Herath, M. Ahmad, M. Al-Wabel, Y.S. Ok, A. Usman, A. Abduljabbar, M. Vithanage, Equilibrium and kinetic mechanisms of woody biochar on aqueous glyphosate removal, Chemosphere 144 (2016) 2516–2521.

[11] A. Wathukarage, I. Herath, M.C.M. Iqbal, M. Vithanage, Mechanistic understanding of crystal violet dye sorption by woody biochar: implications for wastewater treatment, Environ. Geochem. Health (2017).

[12] D. Mohan, A. Sarswat, Y.S. Ok, C.U. Pittman, Organic and inorganic contaminants removal from water with biochar, a renewable, low cost and sustainable adsorbent – a critical review, Bioresour. Technol. 160 (2014) 191–202.

[13] C.E. Brewer, Biochar Characterization and Engineering, Iowa State University, 2012.

[14] M. Sevilla, R. Mokaya, Energy storage applications of activated carbons: supercapacitors and hydrogen storage, Energy Environ. Sci. 7 (2014) 1250–1280.

[15] N. Anderson, J.G. Jones, D. Page-Dumroese, D. McCollum, S. Baker, D. Loeffler, W. Chung, A comparison of producer gas, biochar, and activated carbon from two distributed scale thermochemical conversion systems used to process forest biomass, Energies 6 (2013).

[16] M. Ahmad, D.H. Moon, M. Vithanage, A. Koutsospyros, S.S. Lee, J.E. Yang, S.E. Lee, C. Jeong, Y.S. Oka, Production and use of biochar from buffalo-weed (Ambrosia trifida L.) for trichloroethylene removal from water, J. Chem. Technol. Biotechnol. 89 (2013) 150–157.

[17] B.A. McCarl C. Peacocke R. Chrisman C.C. Kung R.D. Sands Economics of biochar production, utilization and greenhouse gas offsets, L. J., J. A.S. (Eds.) Biochar for Environmental Management: Science and Technology, Earthscan, London, 2009, pp. 341–358.

[18] M.B. Ahmed, J.L. Zhou, H.H. Ngo, W. Guo, M. Chen, Progress in the preparation and application of modified biochar for improved contaminant removal from water and wastewater, Bioresour. Technol. 214 (2016) 836–851.

[19] A.U. Rajapaksha, S.S. Chen, D.C.W. Tsang, M. Zhang, M. Vithanage, S. Mandal, B. Gao, N.S. Bolan, Y.S. Ok, Engineered/designer biochar for contaminant removal/immobilization from soil and water: potential and implication of biochar modification, Chemosphere 148 (2016) 276–291.

[20] S. Mandal, B. Sarkar, N. Bolan, J. Novak, Y.S. Ok, L. Van Zwieten, B.P. Singh, M.B. Kirkham, G. Choppala, K. Spokas, R. Naidu, Designing advanced biochar products for maximizing greenhouse gas mitigation potential, Crit. Rev. Environ. Sci. Technol. 46 (2016) 1367–1401.

[21] Y. Yao, B. Gao, J. Fang, M. Zhang, H. Chen, Y. Zhou, A.E. Creamer, Y. Sun, L. Yang, Characterization and environmental applications of clay–biochar composites, Chem. Eng. J. 242 (2014) 136–143.

[22] E. Fosso-Kankeu, F.B. Waanders, F.W. Steyn, The preparation and characterization of clay-biochar composites for the removal of metal pollutants, Pretoria (South Africa), 7th International Conference on Latest Trends in Engineering & TechnologyIrene, (2015).

[23] M. Zhang, B. Gao, Y. Yao, Y. Xue, M. Inyang, Synthesis of porous MgO-biochar nanocomposites for removal of phosphate and nitrate from aqueous solutions, Chem. Eng. J. 210 (2012) 26–32.

[24] M.I. Inyang, B. Gao, Y. Yao, Y. Xue, A. Zimmerman, A. Mosa, P. Pullammanappallil, Y.S. Ok, X. Cao, A review of biochar as a low-cost adsorbent for aqueous heavy metal removal, Crit. Rev. Environ. Sci. Technol. 46 (2016) 406–433.

[25] C. Peiris, S.R. Gunatilake, T.E. Mlsna, D. Mohan, M. Vithanage, Biochar based removal of antibiotic sulfonamides and tetracyclines in aquatic environments: a critical review, Bioresour. Technol. 246 (2017) 150–159.

[26] W.-J. Liu, H. Jiang, H.-Q. Yu, Development of biochar-based functional materials: toward a sustainable platform carbon material, Chem. Rev. 115 (2015) 12251–12285.

[27] B. Wang, B. Gao, J. Fang, Recent advances in engineered biochar productions and applications, Crit. Rev. Environ. Sci. Technol. 47 (2017) 2158–2207.

[28] M. Vithanage, I. Herath, S. Joseph, J. Bundschuh, N. Bolan, Y.S. Ok, M.B. Kirkham, J. Rinklebe, Interaction of arsenic with biochar in soil and water: a critical review, Carbon 113 (2017) 219–230.

[29] Y. Deng, T. Zhang, Q. Wang, Biochar adsorption treatment for typical pollutants removal in livestock wastewater: a review, in: W.-J. Huang (Ed.), Engineering Applications of Biochar, InTech, Rijeka, 2017, p. Ch. 05.

[30] F.R. Oliveira, A.K. Patel, D.P. Jaisi, S. Adhikari, H. Lu, S.K. Khanal, Environmental application of biochar: current status and perspectives, Bioresour. Technol. 246 (2017) 110–122.

[31] J.M. Patra, S.S. Panda, N.K. Dhal, Biochar as a low-cost adsorbent for heavy metal removal: a review, Int. J. Res. BioSci. 5 (2016) 1–7.

[32] X.-F. Tan, Y.-G. Liu, Y.-L. Gu, Y. Xu, G.-M. Zeng, X.-J. Hu, S.-B. Liu, X. Wang, S.-M. Liu, J. Li, Biochar-based nano-composites for the decontamination of wastewater: a review, Bioresour. Technol. 212 (2016) 318–333.

[33] T. Xie, K. Reddy, C. Wang, E. Yargicoglu, K. Spokas, Characteristics and applications of biochar for environmental remediation: a review, Crit. Rev. Environ. Sci. Technol. 45 (2014) 939–969.

[34] O.D. Nartey, B. Zhao, Biochar preparation, characterization, and adsorptive capacity and its effect on bioavailability of contaminants: an overview, Adv. Mater. Sci. Eng. 2014 (2014) 12.

[35] S.D. Gisi, M. Notarnicola, Characteristics and adsorption capacities of low-cost sorbents for waste water treatment: a review, Sustain. Mater. Technol. 9 (2016) 10–40.

[36] H. Zhang, Z. Yu, Q. Huang, A review: utilization of biochar for wastewater treatment, in: A. Bhatnagar (Ed.), Application of Adsorbents for Water Pollution Control, Bentham Science, 2018, pp. 413–431.

[37] M. Inyang, E. Dickenson, The potential role of biochar in the removal of organic and microbial contaminants from potable and reuse water: a review, Chemosphere 134 (2015) 232–240.

[38] E. Rosales, J. Meijide, M. Pazos, M.A. Sanromán, Challenges and recent advances in biochar as low-cost biosorbent: from batch assays to continuous-flow systems, Bioresour. Technol. 246 (2017) 176–192.

[39] S. Brick, W. Madison, Biochar: Assessing the Promise and Risks To Guide U.S. Policy, in: N.R.D. Council (Ed.), 2010.

[40] S. Brick, S. Lyutse, Biochar: Assessing the promise and risks to guide US policy, (2010).

[41] A. Enders, K. Hanley, T. Whitman, S. Joseph, J. Lehmann, Characterization of biochars to evaluate recalcitrance and agronomic performance, Bioresour. Technol. 114 (2012) 644–653.

[42] S.P. Sohi, E. Krull, E. Lopez-Capel, R. Bol, Chapter 2 – A Review of Biochar and its Use and Function in Soil, Advances in Agronomy, Academic Press, 2010, pp. 47–82.

[43] K.B. Cantrell, P.G. Hunt, M. Uchimiya, J.M. Novak, K.S. Ro, Impact of pyrolysis temperature and manure source on physicochemical characteristics of biochar, Bioresour. Technol. 107 (2012) 419–428.

[44] J. Lee, D. Choi, Y.S. Ok, S.-R. Lee, E.E. Kwon, Enhancement of energy recovery from chicken manure by pyrolysis in carbon dioxide, J. Clean. Prod. 164 (2017) 146–152.

[45] J. Bourke, M.M. Harris, C. Fushimi, T. Nunoura, M.J. Antal Jr., Do all carbonized charcoals have the same chemical structure? 2. A model of the chemical structure of carbonized charcoal, Ind. Eng. Chem. Res. 46 (2007) 5954–5967.

[46] S.-R. Lee, J. Lee, T. Lee, Y.F. Tsang, K.-H. Jeong, J.-I. Oh, E.E. Kwon, Strategic use of CO_2 for co-pyrolysis of swine manure and coal for energy recovery and waste disposal, J. CO_2 Util. 22 (2017) 110–116.

[47] X. Yang, H. Wang, J. Strong, S. Xu, S. Liu, K. Lu, K. Sheng, J. Guo, L. Che, L. He, Y. S. Ok, G. Yuan, Y. Shen, X. Chen, Thermal properties of biochars derived from waste biomass generated by agricultural and forestry sectors, 2017.

[48] X. Gai, H. Wang, J. Liu, L. Zhai, S. Liu, T. Ren, H. Liu, Effects of feedstock and pyrolysis temperature on biochar adsorption of ammonium and nitrate, PLoS One 9 (2014) e113888.

[49] G. Yang, L. Wu, Q. Xian, F. Shen, J. Wu, Y. Zhang, Removal of congo red and methylene blue from aqueous solutions by vermicompost-derived biochars, PLoS One 11 (2016) e0154562.

[50] X. Cao, W. Harris, Properties of dairy-manure-derived biochar pertinent to its potential use in remediation, Bioresour. Technol. 101 (2010) 5222–5228.

[51] M. Ahmad, S.S. Lee, A.U. Rajapaksha, M. Vithanage, M. Zhang, J.S. Cho, S.-E. Lee, Y.S. Ok, Trichloroethylene adsorption by pine needle biochars produced at various pyrolysis temperatures, Bioresour. Technol. 143 (2013) 615–622.

[52] A. Rawal, S.D. Joseph, J.M. Hook, C.H. Chia, P.R. Munroe, S. Donne, Y. Lin, D. Phelan, D.R.G. Mitchell, B. Pace, J. Horvat, J.B.W. Webber, Mineral–biochar composites: molecular structure and porosity, Environ. Sci. Technol. 50 (2016) 7706–7714.
[53] M.I. Al-Wabel, A. Al-Omran, A.H. El-Naggar, M. Nadeem, A.R.A. Usman, Pyrolysis temperature induced changes in characteristics and chemical composition of biochar produced from conocarpus wastes, Bioresour. Technol. 131 (2013) 374–379.
[54] A.U. Rajapaksha, M. Vithanage, M. Ahmad, D.-C. Seo, J.-S. Cho, S.-E. Lee, S.S. Lee, Y.S. Ok, Enhanced sulfamethazine removal by steam-activated invasive plant-derived biochar, J. Hazard. Mater. 290 (2015) 43–50.
[55] J.-H. Yuan, R.-K. Xu, H. Zhang, The forms of alkalis in the biochar produced from crop residues at different temperatures, Bioresour. Technol. 102 (2011) 3488–3497.
[56] M. Li, Z. Zhao, X. Wu, W. Zhou, L. Zhu, Impact of mineral components in cow manure biochars on the adsorption and competitive adsorption of oxytetracycline and carbaryl, RSC Adv. 7 (2017) 2127–2136.
[57] B. Chen, Z. Chen, Sorption of naphthalene and 1-naphthol by biochars of orange peels with different pyrolytic temperatures, Chemosphere 76 (2009) 127–133.
[58] B. Chen, D. Zhou, L. Zhu, Transitional adsorption and partition of nonpolar and polar aromatic contaminants by biochars of pine needles with different pyrolytic temperatures, Environ. Sci. Technol. 42 (2008) 5137–5143.
[59] A. Solanki, T.H. Boyer, Pharmaceutical removal in synthetic human urine using biochar, Environ. Sci. Water Res. Technol. 3 (2017) 553–565.
[60] Y. Gao, Y. Li, L. Zhang, H. Huang, J. Hu, S.M. Shah, X. Su, Adsorption and removal of tetracycline antibiotics from aqueous solution by graphene oxide, J. Colloids Interface Sci. 368 (2012) 540–546.
[61] P.H. Chang, Z. Li, J.S. Jean, W.T. Jiang, Q. Wu, C.Y. Kuo, J. Kraus, Desorption of tetracycline from montmorillonite by aluminum, calcium, and sodium: an indication of intercalation stability, Int. J. Environ. Sci. Technol. 11 (2014) 633–644.
[62] P.-H. Chang, W.-T. Jiang, Z. Li, C.-Y. Kuo, Q. Wu, J.-S. Jean, G. Lv, Interaction of ciprofloxacin and probe compounds with palygorskite PFl-1, J. Hazard. Mater. 303 (2016) 55–63.
[63] X. Han, C.-F. Liang, T.-Q. Li, K. Wang, H.-G. Huang, X.-E. Yang, Simultaneous removal of cadmium and sulfamethoxazole from aqueous solution by rice straw biochar, J. Zhejiang Univ. Sci. B 14 (2013) 640–649.
[64] V. Vimonses, S. Lei, B. Jin, C.W.K. Chow, C. Saint, Adsorption of congo red by three Australian kaolins, Appl. Clay Sci. 43 (2009) 465–472.
[65] R. Pusch, Bentonite Cay: Environmental Properties and Applications, CRC Press, Boca Raton, FL, USA, 2015.
[66] L. Aristilde, B. Lanson, J. Miéhé-Brendlé, C. Marichal, L. Charlet, Enhanced interlayer trapping of a tetracycline antibiotic within montmorillonite layers in the presence of Ca and Mg, J. Colloids Interface Sci. 464 (2016) 153–159.
[67] A.U. Rajapaksha, M. Vithanage, L. Jayarathna, C.K. Kumara, Natural red earth as a low cost material for arsenic removal: kinetics and the effect of competing ions, Appl. Geochem. 26 (2011) 648–654.
[68] R. Donat, A. Akdogan, E. Erdem, H. Cetisli, Thermodynamics of Pb^{2+} and Ni^{2+} adsorption onto natural bentonite from aqueous solutions, J. Colloids Interface Sci. 286 (2005) 43–52.
[69] M.K. Uddin, A review on the adsorption of heavy metals by clay minerals, with special focus on the past decade, Chem. Eng. J. 308 (2017) 438–462.
[70] A.A. Adeyemo, I.O. Adeoye, O.S. Bello, Adsorption of dyes using different types of clay: a review, Appl. Water Sci. 7 (2017) 543–568.
[71] G. Dou, J.L. Goldfarb, In situ upgrading of pyrolysis biofuels by bentonite clay with simultaneous production of heterogeneous adsorbents for water treatment, Fuel 195 (2017) 273–283.
[72] S. Ismadji, D.S. Tong, F.E. Soetaredjo, A. Ayucitra, W.H. Yu, C.H. Zhou, Bentonite hydrochar composite for removal of ammonium from Koi fish tank, Appl. Clay Sci. 119 (2016) 146–154.
[73] L. Chen, X.L. Chen, C.H. Zhou, H.M. Yang, S.F. Ji, D.S. Tong, Z.K. Zhong, W.H. Yu, M.Q. Chu, Environmental-friendly montmorillonite-biochar composites: Facile production and tunable adsorption-release of ammonium and phosphate, J. Clean. Prod. 156 (2017) 648–659.
[74] V. Frišták, B. Michálek ová-Richveisová, E. Víglašová, L. Ďuriška, M. Galamboš, E. Moreno-Jimenéz, M. Pipíška, G. Soja, Sorption separation of Eu and As from single-component systems by Fe-modified biochar: kinetic and equilibrium study, J. Iran. Chem. Soc. 14 (2017) 521–530.
[75] N. Chaukura, E.C. Murimba, W. Gwenzi, Synthesis, characterisation and methyl orange adsorption capacity of ferric oxide–biochar nano-composites derived from pulp and paper sludge, Appl. Water Sci. 7 (2017) 2175–2186.
[76] C.-H. Ooi, Y.-L. Sim, F.-Y. Yeoh, Urea adsorption by activated carbon prepared from palm kernel shell, AIP Conf. Proc. 1865 (2017) 020009.
[77] M.C. Wang, G.D. Sheng, Y.P. Qiu, A novel manganese-oxide/biochar composite for efficient removal of lead(II) from aqueous solutions, Int. J. Environ. Sci. Technol. 12 (2015) 1719–1726.
[78] Y. Zhou, B. Gao, A.R. Zimmerman, H. Chen, M. Zhang, X. Cao, Biochar-supported zerovalent iron for removal of various contaminants from aqueous solutions, Bioresour. Technol. 152 (2014) 538–542.
[79] J. Tang, H. Lv, Y. Gong, Y. Huang, Preparation and characterization of a novel graphene/biochar composite for aqueous phenanthrene and mercury removal, Bioresour. Technol. 196 (2015) 355–363.
[80] B. Sarkar, S. Mandal, Y.F. Tsang, P. Kumar, K.-H. Kim, Y.S. Ok, Designer carbon nanotubes for contaminant removal in water and wastewater: a critical review, Sci. Total Environ. 612 (2018) 561–581.
[81] Y. Zhou, B. Gao, A.R. Zimmerman, J. Fang, Y. Sun, X. Cao, Sorption of heavy metals on chitosan-modified biochars and its biological effects, Chem. Eng. J. 231 (2013) 512–518.
[82] T. Liu, B. Gao, J. Fang, B. Wang, X. Cao, Biochar-supported carbon nanotube and graphene oxide nanocomposites for Pb(ii) and Cd(ii) removal, RSC Adv. 6 (2016) 24314–24319.
[83] Y. Li, Z. Wang, X. Xie, J. Zhu, R. Li, T. Qin, Removal of Norfloxacin from aqueous solution by clay-biochar composite prepared from potato stem and natural attapulgite, Colloids Surf. A 514 (2017) 126–136.
[84] B. Zhao, D. O'Connor, J. Zhang, T. Peng, Z. Shen, D.C.W. Tsang, D. Hou, Effect of pyrolysis temperature, heating rate, and residence time on rapeseed stem derived biochar, J. Clean. Prod. 174 (2018) 977–987.
[85] J.M. Novak, I. Lima, B. Xing, J.W. Gaskin, C. Steiner, K.C. Das, M. Ahmedna, D. Rehrah, D.W. Watts, W.J. Busscher, H. Schomberg, Characterization of designer biochar produced at different temperatures and their effects on a loamy sand, Ann. Environ. Sci. 3 (2009) 195–206.
[86] F. Lian, F. Huang, W. Chen, B. Xing, L. Zhu, Sorption of apolar and polar organic contaminants by waste tire rubber and its chars in single- and bi-solute systems, Environ. Pollut. 159 (2011) 850–857.
[87] S. Wang, B. Gao, A.R. Zimmerman, Y. Li, L. Ma, W.G. Harris, K.W. Migliaccio, Removal of arsenic by magnetic biochar prepared from pinewood and natural hematite, Bioresour. Technol. 175 (2015) 391–395.
[88] K. Komnitsas, D. Zaharaki, Morphology of modified biochar and its potential for phenol removal from aqueous solutions, Environ. Sci. Technol. 4 (2016).
[89] D. Angın, Effect of pyrolysis temperature and heating rate on biochar obtained from pyrolysis of safflower seed press cake, Bioresour. Technol. 128 (2013) 593–597.
[90] M.S. Nazir, M.H. Mohamad Kassim, L. Mohapatra, M.A. Gilani, M.R. Raza, K. Majeed, Characteristic properties of manoclays and characterization of nanoparticulates and nanocomposites, in: M. Jawaid, A.e.K. Qaiss, R. Bouhfid (Eds.), Nanoclay Reinforced Polymer Composites: Nanocomposites and Bionanocomposites, Springer Singapore, Singapore, 2016, pp. 35–55.
[91] Y. Yao, Sorption of Phosphate and Other Contaminants on Biochar and its Environmental Implications, University of Florida, 2013.
[92] Y. Yao, B. Gao, M. Inyang, A.R. Zimmerman, X. Cao, P. Pullammanappallil, L. Yang, Removal of phosphate from aqueous solution by biochar derived from anaerobically digested sugar beet tailings, J. Hazard. Mater. 190 (2011) 501–507.
[93] K. Lou, A.U. Rajapaksha, Y.S. Ok, S.X. Chang, Pyrolysis temperature and steam activation effects on sorption of phosphate on pine sawdust biochars in aqueous solutions, Chem. Speciat. Bioavailab. 28 (2016) 42–50.
[94] T. Almeelbi, A. Bezbaruah, Aqueous phosphate removal using nanoscale zero-valent iron, J. Nanopart. Res. 14 (2012) 900.
[95] T. Tuutijärvi, J. Lu, M. Sillanpää, G. Chen, As(V) adsorption on maghemite nanoparticles, J. Hazard. Mater. 166 (2009) 1415–1420.
[96] G. Li, B. Shen, F. Li, L. Tian, S. Singh, F. Wang, Elemental mercury removal using biochar pyrolyzed from municipal solid waste, Fuel Process. Technol. 133 (2015) 43–50.
[97] E. Fosso-Kankeu, F.B. Waanders, J. Potgieter, Enhanced adsorption capacity of sweet sorghum derived biochar towards malachite green dye using bentonite clay, International Conference on Advances in Science, Engineering, Technology and Natural ResourcesParys (South Africa), (2016).
[98] E. Agrafioti, D. Kalderis, E. Diamadopoulos, Ca and Fe modified biochars as adsorbents of arsenic and chromium in aqueous solutions, J. Environ. Manage. 146 (2014) 444–450.
[99] H. Zhang, Z. Wang, R. Li, J. Guo, Y. Li, J. Zhu, X. Xie, TiO2 supported on reed straw biochar as an adsorptive and photocatalytic composite for the efficient degradation of sulfamethoxazole in aqueous matrices, Chemosphere 185 (2017) 351–360.
[100] C. Gerente, V.K.C. Lee, P.L. Cloirec, G. McKay, Application of chitosan for the removal of metals from wastewaters by adsorption—mechanisms and models review, Crit. Rev. Environ. Sci. Technol. 37 (2007) 41–127.
[101] M. Inyang, B. Gao, A. Zimmerman, M. Zhang, H. Chen, Synthesis, characterization, and dye sorption ability of carbon nanotube–biochar nanocomposites, Chem. Eng. J. 236 (2014) 39–46.
[102] L. Zhou, Y. Huang, W. Qiu, Z. Sun, Z. Liu, Z. Song, Adsorption properties of Nano-MnO2–biochar composites for copper in aqueous solution, Molecules 22 (2017) 173.
[103] D. Kołodyńska, J. Bąk, Use of three types of magnetic biochar in the removal of copper(II) ions from wastewaters, Sep. Sci. Technol. 53 (2018) 1045–1057.
[104] M.L. Sanyang, W.A.W.A.K. Ghani, A. Idris, M.B. Ahmad, Hydrogel biochar composite for arsenic removal from wastewater, Desalin. Water Treat. 57 (2016) 3674–3688.
[105] L. Yan, L. Kong, Z. Qu, L. Li, G. Shen, Magnetic biochar decorated with ZnS nanocrytals for Pb (II) removal, ACS Sustain. Chem. Eng. 3 (2015) 125–132.
[106] L.-L. Ling, W.-J. Liu, S. Zhang, H. Jiang, Magnesium oxide embedded nitrogen self-doped biochar composites: fast and high-efficiency adsorption of heavy metals in an aqueous solution, Environ. Sci. Technol. 51 (2017) 10081–10089.
[107] W. Liu, J. Zhang, C. Zhang, L. Ren, Sorption of norfloxacin by lotus stalk-based activated carbon and iron-doped activated alumina: mechanisms, isotherms and kinetics, Chem. Eng. J. 171 (2011) 431–438.
[108] A.G. Trovo, R.F. Nogueira, A. Aguera, C. Sirtori, A.R. Fernandez-Alba, Photodegradation of sulfamethoxazole in various aqueous media: persistence, toxicity and photoproducts assessment, Chemosphere 77 (2009) 1292–1298.
[109] H. Wu, Q. Feng, P. Lu, M. Chen, H. Yang, Degradation mechanisms of cefotaxime using biochar supported Co/Fe bimetallic nanoparticles, Environ. Sci. Water Res. Technol. 4 (2018) 964–975.
[110] J. Farrell, M. Kason, N. Melitas, T. Li, Investigation of the long-term performance

of zero-valent iron for reductive dechlorination of trichloroethylene, Environ. Sci. Technol. 34 (2000) 514–521.
[111] X. Weng, Q. Sun, S. Lin, Z. Chen, M. Megharaj, R. Naidu, Enhancement of catalytic degradation of amoxicillin in aqueous solution using clay supported bimetallic Fe/Ni nanoparticles, Chemosphere 103 (2014) 80–85.
[112] K. Miyajima, C. Noubactep, Effects of mixing granular iron with sand on the efficiency of methylene blue discoloration, Chem. Eng. J. 200–202 (2012) 433–438.
[113] L. Han, S. Xue, S. Zhao, J. Yan, L. Qian, M. Chen, Biochar supported nanoscale iron particles for the efficient removal of methyl orange dye in aqueous solutions, PLoS One 10 (2015) e0132067.
[114] A. Naeem, P. Westerhoff, S. Mustafa, Vanadium removal by metal (hydr)oxide adsorbents, Water Res. 41 (2007) 1596–1602.
[115] S. Kara, C. Aydiner, E. Demirbas, M. Kobya, N. Dizge, Modeling the effects of adsorbent dose and particle size on the adsorption of reactive textile dyes by fly ash, Desalination 212 (2007) 282–293.
[116] H. Zhang, C.-H. Huang, Adsorption and oxidation of fluoroquinolone antibacterial agents and structurally related amines with goethite, Chemosphere 66 (2007) 1502–1512.
[117] W. Wu, H. Wang, J. Xu, Z. Xie, Adsorption characteristic of bensulfuron-methyl at variable added Pb^{2+} concentrations on paddy soils, J. Environ. Sci. 21 (2009) 1129–1134.
[118] B. Peng, L. Chen, C. Que, K. Yang, F. Deng, X. Deng, G. Shi, G. Xu, M. Wu, Adsorption of antibiotics on graphene and biochar in aqueous solutions induced by π-π interactions, Sci. Rep. 31920 (2016).
[119] A.A. Bazrafshan, S. Hajati, M. Ghaedi, Synthesis of regenerable $Zn(OH)_2$ nanoparticle-loaded activated carbon for the ultrasound-assisted removal of malachite green: optimization, isotherm and kinetics, RSC Adv. 5 (2015) 79119–79128.
[120] T.H. Nguyen, H.-H. Cho, D.L. Poster, W.P. Ball, Evidence for a pore-filling mechanism in the adsorption of aromatic hydrocarbons to a natural wood char, Environ. Sci. Technol. 41 (2007) 1212–1217.